Theoretical and computational methods for the noninvasive detection of gastric electrical source coupling

Andrei Irimia* and L. Alan Bradshaw†
Living State Physics Laboratories, Department of Physics and Astronomy, Vanderbilt University, Nashville, Tennessee, 37235, USA
(Received 23 November 2003; published 28 May 2004)

The ability to study the pathology of the stomach noninvasively from magnetic field measurements is important due to the significant practical advantages offered by noninvasive methods over other techniques of investigation. The inverse biomagnetic problem can play a central role in this process due to the information that inverse solutions can yield concerning the characteristics of the gastric electrical activity (GEA). To analyze gastrointestinal (GI) magnetic fields noninvasively, we have developed a computer implementation of a least-squares minimization algorithm that obtains numerical solutions to the biomagnetic inverse problem for the stomach. In this paper, we show how electric current propagation and the mechanical coupling of gastric smooth muscle cells during electrical control activity can be studied using such solutions. To validate our model, two types of numerical simulations of the GEA were developed and successfully used to demonstrate the ability of our computer algorithm to detect and accurately analyze these two phenomena. We also describe our analysis of experimental, noninvasively acquired gastric biomagnetic data as well as the information of interest that our numerical method can yield in clinical studies. Most importantly, we present experimental evidence that the coupling of gastric electrical sources can be observed using noninvasive techniques of measurement, in our case with the use of a superconducting quantum interference device magnetometer. We discuss the relevance and implications of our achievement to the future of GI research.

DOI: 10.1103/PhysRevE.69.051920 PACS number(s): 87.19.Nn, 87.17.Aa, 87.10.+e

I. INTRODUCTION AND PURPOSE

The subject of noninvasive biomagnetic measurements has received a considerable amount of attention in light of the latest developments in the field of biophysical research. In particular, the development of reliable methods for solving the inverse biomagnetic problem has increased the attention devoted to the analysis of magnetic fields originating in the human stomach in an attempt to better understand the mechanisms at work in this organ. Noninvasive biomagnetic measurement studies have recently been conducted [1–3,6–8] in order to assess the characteristics of the gastric electrical activity (GEA), especially as it relates to the diagnosis of pathological states in humans and animals.

Numerous theoretical and computational models of the electrical activity in the stomach have been developed [9–18]. The GEA is generated due to the periodic depolarization and repolarization of stomach cells and it manifests itself as a wave propagating aborally from the gastric corpus toward the pylorus. In the quasistatic approximation, the phenomenon can be modeled as one or several current dipoles propagating through the electric syncytium of the stomach. Anomalies in the characteristics of this propagation have been studied and their relevance to the field of medical diagnosis has also been the focus of active research. In particular, the use of superconducting quantum interference device (SQUID) magnetometers has proven to be very suitable for detecting and studying the GEA in both healthy and diseased subjects. An important practical aspect in favor of using SQUIDs for experimental biological data acquisition is the ability to study gastrointestinal (GI) electromagnetic phenomena noninvasively, which greatly eases the task of conducting clinical studies. Moreover, noninvasive GEA studies are encouraging in light of current efforts to identify effective ways of analyzing the phenomenon of abnormal current propagation, which is associated with pathological conditions such as gastroparesis and ischemia.

In this article, we describe our noninvasive analysis of the GEA in humans from magnetic fields recorded with SQUID magnetometers. Most importantly, we here report our ability to detect electric signal coupling in the stomach using noninvasive methods of measurement by employing a least-squares approximation algorithm for solving the biomagnetic inverse problem.

II. FORWARD AND INVERSE MODELS

In the human body, biomagnetic fields arise due to electric currents in various types of tissue that can be assumed to be homogeneous; in studies of gastric biomagnetism, the medium of current propagation consists of gastric smooth muscle cells. In order to investigate the GEA from noninvasive magnetic field measurements, a number of theoretical concepts must be applied to the mathematical modeling of this phenomenon. One of these involves solving the so-called biomagnetic inverse problem, which consists of employing the mathematical tools of the quasistatic approximation to determine a current density **J** based on known values of the magnetic field **B**. This is typically performed using the law of Biot and Savart written in a well-chosen form, according to the specifications of the practical problem to which it is applied. A large section of biophysical modeling and signal

*Electronic address: andrei.irimia@vanderbilt.edu
†Electronic address: alan.bradshaw@vanderbilt.edu

processing literature has been devoted to this subject due to its importance in various areas of biophysics, including GI research.

Solving the inverse problem requires a thorough understanding of the forward problem, which consists of computing the magnetic field **B** using experimental measurements and/or *a priori* knowledge of the electric potential V and gastric current density **J**. Quasistatically, a current dipole **Q** approximates a localized electric current [19] and can be thought of as a concentration of a primary (as opposed to Ohmic) current $\mathbf{J}_p(\mathbf{r}')$ to a single point, i.e.,

$$\mathbf{J}_p(\mathbf{r}') = \mathbf{Q}\delta(\mathbf{r} - \mathbf{r}'), \tag{1}$$

where we employed the Dirac delta function $\delta(\mathbf{r}-\mathbf{r}')$. In this notation, the vector $\mathbf{r}'$ extends from the origin of the coordinate system to the position of the localized current, while **r** identifies the point where the magnetic field **B** is recorded. For radial fields, given the distribution of electric currents in the abdomen, the expression for the magnetic field due to these currents can be written, according to the theoretical model and derivations of Ilmoniemi *et al.* [20], in the form

$$\mathbf{B}(\mathbf{r}) = \frac{\mu_0}{4\pi}\int\int_{\Omega}\int \frac{1}{|\mathbf{r}-\mathbf{r}'|^3}\mathbf{J}_p(\mathbf{r}')\times(\mathbf{r}-\mathbf{r}')d^3\mathbf{r}', \tag{2}$$

where Ω is the volume of the abdomen modeled as a horizontally layered conductor. To identify current distributions from information contained in magnetic field recordings, one can determine the location, orientation, and time evolution of electric current dipoles accounting for experimentally acquired **B** field values. This task requires realistic, though not unique, solutions to the inverse problem. The existence of more than one such solution accounting for the recorded field is due to the presence of magnetically silent sources, which can greatly complicate the task of solving this problem, although appropriate anatomical constraints can allow the identification of realistic solutions.

In our experimental investigations involving humans, the input coils of the SQUID magnetometer are positioned above the abdomen of the patient and possess the ability to detect magnetic fields whose sources are located in both the stomach and the intestine. For this reason, in the data acquisition experiments that make the object of our present study, one can assume that the source of the gastric electric current producing the magnetic field **B** is located in a homogeneous medium, while the measurement coils of the SQUID magnetometer are positioned immediately above the body of the patient.

If the simplifying assumption is made that the abdomen and the space above it are separated by an infinite half plane, the equation for the magnetic field outside the body due to an electric dipole in this homogeneous medium can be written as

$$\mathbf{B} = \frac{\mu_0}{4\pi}\frac{1}{|\mathbf{r}-\mathbf{r}'|^3}\mathbf{Q}\times(\mathbf{r}-\mathbf{r}'). \tag{3}$$

Since Eqs. (2) and (3) are valid only for radial **B** fields, volume currents at conductor boundaries must also be incorporated for nonradial fields; otherwise, the model is valid only inside the homogeneous conductor. Thus, for noninvasive measurements made outside the body and normal to the surface that separates the two media (which is the case in our experiments), the equation above is valid only for the radial component of the magnetic field, i.e., the component in the $\hat{\mathbf{k}}$ direction [21,22]:

$$B_z = \frac{\mu_0}{4\pi}\frac{1}{|\mathbf{r}-\mathbf{r}'|^3}[Q_x(y-y') - Q_y(x-x')], \tag{4}$$

where the $\hat{\mathbf{k}}$ direction is normal to the surface of the abdomen and directed upward, assuming that the subject is in supine position. In the case of our numerical method implementation, we found that computer memory and processor speed limitations increase drastically with the number of inverse dipoles included in the least-squares procedure. Consequently, the assumption was made in the present study that two current dipoles $\mathbf{Q}_1$ and $\mathbf{Q}_2$—one gastric and the other intestinal, respectively—were sufficient to describe the unknown sources of current producing the **B** field detected by the magnetometer. The numerical method used here to identify current dipoles from **B** data consists of performing a least-squares approximation of the current dipole vector components. In this approach, a systematic search is performed within the volume of the abdomen in order to determine the locations of these best-fitting dipoles explaining the **B** data; these assumed positions correspond to nodes (elements) of a dense three-dimensional matrix **M** covering the volume of the abdomen in which the dipoles can be located.

As explained in detail by Sarvas [19], we describe our inverse problem in terms of 12 unknown parameters, namely, the vector components of the two dipoles in the $\hat{\mathbf{i}}$, $\hat{\mathbf{j}}$, and $\hat{\mathbf{k}}$ directions as well as their positions. Moreover, based on anatomical considerations, we assume that each of the gastric and intestinal dipoles can be located only in one of the upper and lower halves of the $\alpha\times\beta\times\gamma$ three-dimensional matrix **M**. In our case, this implies that half of the magnetometer input coils record **B** data above the stomach while the other half record magnetic fields above the intestine. Since the two dipoles are each to be identified within a separate, distinct portion of the three-dimensional (3D) grid, all combinations of dipole locations must be examined. The vector components of each dipole are then determined through the use of the least-squares procedure.

In our case, given a magnetic field experimental data set acquired in a horizontal measurement plane determined by the input coils of the SQUID magnetometer, the least-squares criterion gives the best-fitting dipole orientation that accounts for the **B** data. To find the orientations of $\mathbf{Q}_1$ and $\mathbf{Q}_2$, we rely on minimizing the sum of squares:

$$\sum_{i=1}^{\alpha}\sum_{j=1}^{\beta}[\widetilde{\mathbf{B}}_{ij}(\mathbf{r}) - \mathbf{B}'_{ij}(\mathbf{r}) - \mathbf{B}''_{ij}(\mathbf{r})]^2, \tag{5}$$

where $\mathbf{B}'_{ij}$ and $\mathbf{B}''_{ij}$ are the computed fields due to $\mathbf{Q}_1$ and $\mathbf{Q}_2$ for the ijth node of an $\alpha\times\beta$ search grid **N** (a horizontal slice within **M** for which z is constant, i.e., $z=0$), while $\widetilde{\mathbf{B}}_{ij}$ is the experimental value of the field at the position denoted by the

corresponding node. The horizontal grid **N** to which the minimization process is applied corresponds here to the plane where the magnetometer input coils are located, i.e., to the plane separating the homogeneous medium in which the dipoles are positioned from the air that surrounds it.

Although a possible *a posteriori* error analysis [4] of our algorithm has not yet been performed, a statistical validation study of our method has already been undertaken [5]. In this study, it was concluded that, if the GI electrical activity is modeled using a current dipole model, only two such dipoles are necessary to account for the magnetic data recorded using a SQUID magnetometer above the human abdomen. We refer the reader to the original article in [5] for further clarification and for an extensive derivation and discussion of our theoretical model.

III. SPATIOTEMPORAL SIMULATIONS

To verify our ability to analyze the GEA using the theoretical and computational model described above, a computer program was developed with the purpose of identifying intestinal and gastric dipoles using magnetic field data recorded with SQUID magnetometers. To test the efficiency and reliability of our dipole identification algorithm, we implemented a forward model simulation in MATLAB (Mathworks Inc., Natick, MA, USA), in which sinusoidally varying abdominal dipoles located under the measurement plane were modeled. Following the theoretical principles previously described, these dipoles were assumed to be positioned at realistic depths.

In the first set of such simulations, single dipoles with various orientations, magnitudes, and locations were modeled. In one such simulation, for example, the only vector component (in units of A m) of the simulated current dipole $\mathbf{Q}_s$ at time $t=0$ (s) was given by

$$\mathbf{Q}_s = -\hat{\mathbf{j}}\ \mathrm{A\,m}, \tag{6}$$

with a dipole moment $|\mathbf{Q}_s| \equiv Q_s$ of 1 A m. As in Eq. (1), $\mathbf{Q}$ is given by $\mathbf{J}_p = \mathbf{Q}\delta(\mathbf{r}-\mathbf{r}')$. The position of the dipole under the measurement plane $z=0$ m was chosen to be

$$\mathbf{r}_s' = -0.02\hat{\mathbf{j}} - 0.07\hat{\mathbf{k}}\ \mathrm{m}, \tag{7}$$

for that simulation, where $\mathbf{r}'$, as previously explained, extends from the origin of the coordinate system to the position of the localized current $\mathbf{J}_p$. Given this arrangement, $\mathbf{B}$ field values as would have been sampled by a SQUID magnetometer were computed in a simulation that spanned 1 min of electrical activity. The goal of this first set of simulations was to verify the spatial resolution of our algorithm in the presence of a single source of current.

To ensure the reliability of our computational method for cases where a large number of electric current dipoles were present, we also implemented a second type of spatiotemporal simulation involving abdominal electric sources. The most important purpose of this second simulation was to verify the ability of our algorithm to detect the coupling of gastric electric sources despite the presence of numerous other uncoupled sources. Since this simulation and the theory behind it have already been discussed to a great extent elsewhere [3], we will only briefly summarize them here.

In the second simulation used for testing our inverse procedure, 190 current dipoles were distributed within the three-dimensional matrix $\mathbf{M}$ corresponding to the space occupied by the stomach and small bowel in the abdominal cavity, as explained in the previous section. Within the simulated volume of the stomach, a number of current dipoles were positioned. These depolarization and repolarization dipoles were simulated in pairs, with repolarization dipoles being far weaker than depolarization dipoles, in agreement with the physiological characteristics of the propagation phenomenon. Throughout all simulations, dipole orientations were adjusted to point in the direction of electrical control activity (ECA) propagation, namely, toward the pylorus. Moreover, the time-dependent magnitudes of all these dipoles due to the distribution of transmembrane potential were controlled so that the resulting magnetic field wave forms due to their presence would exhibit the well-known frequency of three cycles min^{-1}. Gastric dipoles were assigned phase shifts from antrum to pylorus of 2π such that the simulated propagation velocity of the GEA across the stomach was 0.33 $\mathrm{cm\,s}^{-1}$.

In all simulations, magnetic field patterns due to the coupled dipoles in the stomach were simulated to migrate from the subject's corpus to the pylorus, in agreement with the characteristics of gastric propagation. Once every 20 s, the patterns reset to the left side of the subject and thus a new gastric wave was generated in the gastric corpus. In addition to the coupling of gastric electrical sources, we also simulated the same phenomenon at the locations of the proximal duodenum and terminal ileum. In each of these two cases, dipoles were oriented along the direction of the GI tract at each of these two locations. Moreover, their magnitudes were adjusted so that the resulting $\mathbf{B}$ wave forms would exhibit a frequency of 12 cycles min^{-1} for the duodenum and 8 cycles min^{-1} for the terminal ileum. These frequency values are all known from previous physiological studies (see [3] and references therein). In addition to the three groups of simulated dipoles described above, namely, those in the stomach, duodenum, and ileum, the remainder of the intestinal dipoles were given random locations and orientations in order to simulate the ECA frequency gradient along the GI tract.

In Fig. 1, we present the spatial distribution of the electric current dipoles simulated by our forward model. The three regions for which periodicity of dipole activity was simulated are each designated by rectangles. As the figure suggests, the positions of dipoles accounting for gastric electrical activity were simulated in a manner that could reproduce the anatomical shape and position of the stomach. These dipoles are located in the uppermost rectangle in Fig. 1, while electrical activity in the duodenum is represented by a series of dipoles located along a curved line in the second rectangle, immediately to the left of the stomach. The third rectangle at the bottom of Fig. 1 designates the positions of dipoles in the ileum for which the periodicity of electrical activity was simulated. The dipoles outside the three areas are those that were assigned random orientations and phase behaviors in our simulation. Simulated magnetic field values

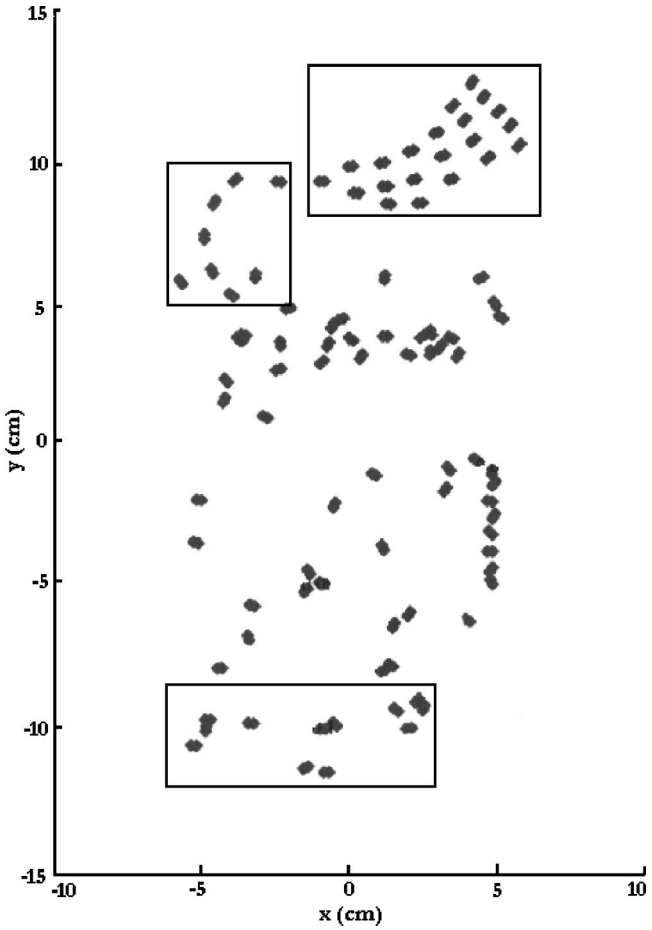

FIG. 1. Spatial distribution of 190 simulated GI electric current dipoles used for inverse procedure testing (units of m). Gastric dipoles are visible at the top of the image, in an arrangement that matches the anatomy of the stomach. Duodenum dipoles are located immediately below, connecting the stomach to the small bowel that covers most of the volume used in the simulation.

due to the electric current dipoles in Fig. 1 were used as input to our inverse problem procedure.

IV. RESULTS AND DISCUSSION

For our single-dipole simulations, we determined the best-fitting location and orientation of one inverse current dipole using the inverse problem algorithm developed. For the example presented in the previous section, the location $\mathbf{r}_i'$ (in m) identified for the inverse-solution dipole $\mathbf{Q}_i$ was found to be

$$\mathbf{r}_i' = -0.006\,\hat{\mathbf{i}} - 0.039\,\hat{\mathbf{j}} - 0.067\,\hat{\mathbf{k}}\ \text{m}. \tag{8}$$

The orientation of the inverse dipole was found to be

$$\mathbf{Q}_i = -0.034\,\hat{\mathbf{i}} - 0.896\,\hat{\mathbf{j}} - 0.202\,\hat{\mathbf{k}}\ \text{A m} \tag{9}$$

with a dipole moment $|\mathbf{Q}_i|$ of 0.9166 A m. Similarly, the orientations of all other simulated dipoles identified using the inverse solution were found to agree with those in the forward model simulation. In the inverse procedure, depolarization and repolarization waves were also reproduced by time variations in the magnitudes of inverse dipoles $\mathbf{Q}_i$. Each GEA temporal wave was found to exhibit an upstroke phase with a sustained repolarization phase, consistent with the known physiology of the GI tract.

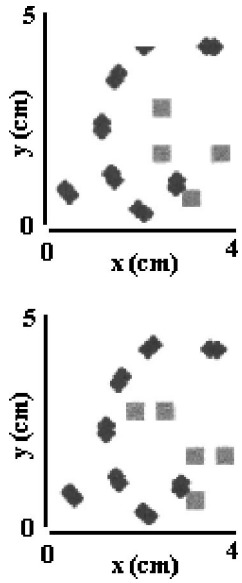

FIG. 2. Simulated (rhombi) and a few inverse (squares) dipoles identified by the least-squares inverse problem algorithm for the anatomical region of the stomach.

Our assumption that each of the gastric and intestinal dipoles is constrained to be located within a specific section of the 3D grid M does not imply that the coils of the instrument cannot record **B** fields produced in the other organ. Such an assumption would be unrealistic not only on anatomical grounds—portions of the intestine can often be located behind the stomach itself—but also because frequencies associated with the electrical activity in the colon spectrally overlap those associated with the stomach. Rather, our assumption concerns only the anatomical *location* of the dipoles being considered, and the spectral overlap between the electrical activities in the stomach and colon is accounted for in a natural manner by the least-squares procedure. This is because, in our approach, both groups of estimated parameters (dipole locations, strengths, and orientations for gastric *and* intestinal sources) are fitted to the **B** field data recorded by *all* input coils, regardless of where the latter are positioned (above the stomach vs intestine) and independent of where the electric sources producing the experimental data are located.

The results of applying our inverse algorithm to the data generated by the forward model with 190 dipoles are shown in Figs. 2–4. The only regions where periodicity of electrical activity was detected were found to be identical to the regions where it had also been simulated in the forward model. Due to the large number of forward model dipoles in the simulation (190 total) and to the fact that we identify only two inverse dipoles per time slice of **B** data generated by the forward model simulation, we believe that studying the time evolution of dipole locations in each region of propagation is the most effective manner of characterizing the spatial resolution and accuracy of our algorithm.

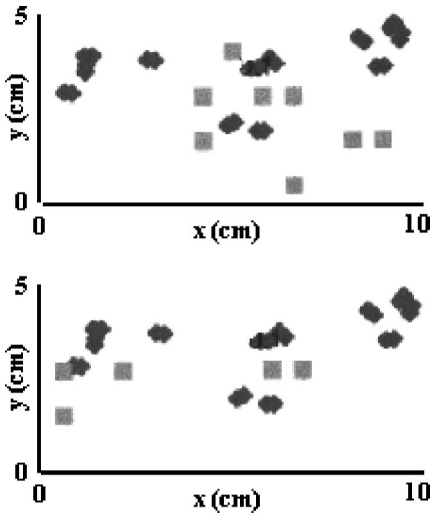

FIG. 3. Same as Fig. 2, but for the duodenum.

Since the number of forward model dipoles is far larger than that of inverse dipoles, we believe that computing the shortest distance between a dipole in the forward model and one found using the inverse model may not always constitute an appropriate way of quantitatively assessing the spatial resolution of our inverse method. This is true because a single inverse dipole accounts for the activity of several dipoles in the forward model simulation. This did not apply to the first simulation we presented here because, in that case, only one inverse dipole was used for identifying the location of one corresponding simulated dipole. Nevertheless, in the case of the simulation with 190 dipoles, it is crucial to reiterate that our algorithm was able to detect propagation only in those regions where the phenomenon had been simulated. To motivate this statement conclusively and persuasively, the locations of several inverse dipoles identified using our algorithm are shown in Figs. 2–4 for each of the three rectangles in Fig. 1, where periodicity was simulated. Each of these three figures demonstrates the spatial resolution of our algorithm for identifying propagation in the stomach, duodenum, and ileum, respectively. In all figures, dark rhombi represent positions of dipoles in the forward model simulation. These locations are identical to those in each rectangle from Fig. 1, but they are presented again in Figs. 2–4 for visual convenience. Squares in Figs. 2–4 represent locations of dipoles identified by the inverse solution as exhibiting electric activity periodicity. Inverse dipoles in images (a) and (b) for each figure correspond to two different, randomly selected, time segments in our simulation. Each inverse dipole, designated by a square, belongs to a different time frame in the magnetic field data. Nevertheless, we found it convenient to show several such dipoles on each figure simply in order to characterize the spatial accuracy of our algorithm both visually and qualitatively. By tracing the locations of such inverse dipoles as functions of time, we were able to identify as regions of current propagation only the areas where this phenomenon was simulated. Consequently, in view of the results obtained with our simulation, we believe that our method is demonstrative of our ability to accurately identify realistic current dipoles and to characterize ECA propagation.

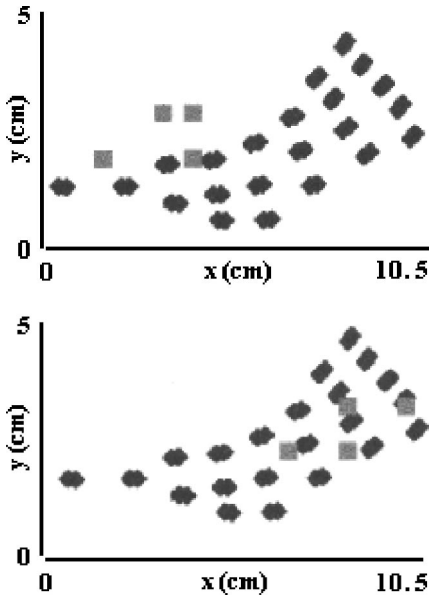

FIG. 4. Same as Fig. 2, but for the ileum.

In addition to analyzing simulated biomagnetic fields, we also used our algorithm to analyze experimental biomagnetic data. Such data were sampled from three healthy human subjects, who were each separately positioned under a Tristan 637i SQUID magnetometer (Tristan Technologies, Inc., San Diego, CA, USA) with their abdomen directly below the input coils of the instrument. The 637i magnetometer in the Living State Physics Laboratories at Vanderbilt University possesses 29 input coils, out of which 19 are distributed around a base with a diameter of 10 in. These 19 input coils record the gradient of the magnetic field along the z axis, which is perpendicular to the abdomen of the subject and oriented upward. The ten other channels record gradients in either one of the $\hat{\mathbf{x}}$ and $\hat{\mathbf{y}}$ directions. Although gradients—rather than magnetic field components—are measured, it is safe to assume that the former are very nearly equal to the latter, because the gradient baseline in our case is 5 cm, which is roughly equal to the source-sensor separation. Simulated gradients would thus be almost identical to simulated fields since only far field sources would contribute substantially.

As a result of applying the inverse problem algorithm with two inverse dipoles [Eq. (5)] to the experimental gastric biomagnetic data, spatial resolution was found to be consistent with *a priori* information offered by the experimental setup, in that regions of anatomical and physiological interest were satisfactorily identified by the inverse solution, as was done in our forward model simulation with 190 dipoles and in previous studies where the spatial resolution of our algorithm was tested [6–8]. The wave forms reconstructed from inverse solutions were all found to exhibit one of the essential characteristics of simulated GEA wave forms, namely, the wave frequency of 3 cycles min^{-1}.

The location where gastric propagation was found to originate according to our inverse solutions was identified in the corpus of the stomach, in agreement with the known characteristics of GEA propagation. As in the forward model simulation presented in the previous section, this result was

obtained by observing the locations of inverse dipoles as a function of time. The position where the ECA was consistently found to originate was thus identified as a pacemaker within the electrical syncytium of the stomach. Using the same method described above, the location where propagation ended was also correctly identified as the pylorus.

The time evolution of the dipole moments associated with the regions of the gastric pacemaker and of the pylorus were found to be of considerable interest. Specifically, applying the inverse algorithm to the human **B** data showed that a high magnitude of the pacemaker dipole was always associated with a low magnitude of the pylorus dipole for every GEA cycle. Moreover, a high magnitude of the pylorus dipole was always associated with a low magnitude of the pacemaker dipole. The change in location of the dipole with the higher magnitude was found to occur at the end of each propagation cycle, such that the electric activity was strongest at the pacemaker location during one cycle, whereafter it was strongest in the pylorus region during the following cycle. This periodic phenomenon, in which the position of the dipole with the higher magnitude alternates betweeen the pylorus and the corpus with each ECA cycle, corresponds to the electric source coupling of these two regions during the GEA and it was observed in all the human subjects analyzed. Thus, our study demonstrates the possibility of observing and describing gastric electrical source coupling using noninvasive techniques of measurement.

We believe that this result is of great interest because it has already been shown that gastric disease states can be simulated by uncoupling source dipoles [17,23]. Our detection of electric source coupling in healthy subjects using solutions to the inverse biomagnetic problem may imply that disease states of the stomach are also detectable using this method. While electric potentials are attenuated by the conductivity of tissues, magnetic fields depend on permeability, which is constant between tissues and almost equal to μ_0. Since it has already been demonstrated that magnetic fields describe internal current sources more accurately than electric fields [1,24], our result shows that it may be possible to indirectly identify states of human gastric disease noninvasively by detecting the uncoupling of electric current sources in the stomach. Moreover, it may also be possible to detect uncoupling using our method by analyzing the time evolution of gastric dipole moments. We believe this to be the case because disease states in the stomach are also associated with the presence of dipoles in distal locations whose frequencies are lower than normal [1–3].

In a previous study by Bradshaw *et al.* [3], a simulation study similar to ours predicted that the electrical activity of uncoupled cells may be associated with inconsistent or retrograde propagation as well as with propagation patterns far less distinct than in the normal stomach; it may also be true that such abnormal behavior is identifiable with our method. However, although experiments are now being conducted in our group to ascertain how noninvasive magnetic field recordings respond to mechanical and pharmacological uncoupling of the stomach, these data are not yet available and a valid conclusion cannot be drawn in this respect at the present time. In [9], we also formulated a theoretical ellipsoidal model capable of reproducing the gastric electric potential and its associated electric field. Since our present computational work predates the theoretical developments therein, more investigative effort is necessary before the applicability of our ellipsoidal model to the present problem is ascertained.

V. CONCLUSIONS

The biomagnetic inverse problem can be of great importance in the process of analyzing the characteristics of GI bioelectric currents. Our method was found to be capable of identifying the locations and orientations of gastric current dipoles due to which magnetic fields are produced in and outside the human abdomen. Most importantly, the coupling of electric sources in the stomach was detected from inverse solutions using data acquired noninvasively. We believe that this achievement is particularly encouraging from the perspective of detecting abnormal current propagation in the future, which may in turn be useful for studying the pathological conditions of the stomach more extensively. We are hopeful that a future study of human patients with abnormal gastric conditions will fully clarify whether inverse solutions to the biomagnetic problem can indeed be used successfully to detect abnormal current propagation in the stomach.

ACKNOWLEDGMENTS

Funding was provided by the Veterans' Affairs Research Service through the National Institute of Health, NIH Grant No. R01 DK 58697-01.

[1] L.A. Bradshaw, W.O. Richards, and J.P. Wikswo, Jr., Med. Biol. Eng. Comput. **39**, 35 (2001).
[2] L.A. Bradshaw, R.S. Wijesinghe, and J.P. Wikswo, Jr., Ann. Biomed. Eng. **29**, 214 (2001).
[3] L.A. Bradshaw, A. Myers, J.P. Wikswo, Jr., and W.O. Richards, IEEE Trans. Biomed. Eng. **50**, 836 (2003).
[4] R.G. Duran, C. Padra, and R. Rodriguez, Math. Models Meth. Appl. Sci. **13**, 1219 (2003).
[5] A. Irimia, J.J. Beauchamp, and L.A. Bradshaw, J. Biol. Phys. (to be published).
[6] A. Irimia and L.A. Bradshaw, in *Proceedings of the IASTED International Conference on Applied Modeling and Simulation* (ACTA Press, Anaheim, CA, 2002), pp. 56–60.
[7] A. Irimia and L.A. Bradshaw, in *Proceedings of the IASTED International Conference on Applied Modeling and Simulation, 2002* (Ref. [6]), pp. 51–55.
[8] A. Irimia, in *Proceedings of the IASTED International Conference on Applied Modeling and Simulation, 2002* (Ref. [6]), pp. 45–50.
[9] A. Irimia and L.A. Bradshaw, Phys. Rev. E **68**, 051905

(2003).
[10] B. Kothapali, IEEE Trans. Biomed. Eng. **39**, 1005 (1992).
[11] N. Mirizzi, R. Stella, and U. Scafoglieri, Med. Biol. Eng. Comput. **24**, 157 (1986).
[12] M.P. Mintchev *et al.*, IEEE Trans. Biomed. Eng. **44**, 1288 (1997).
[13] P.Z. Rashev, M.P. Mintchev, and K.L. Bowes, IEEE Trans. Inf. Technol. Biomed. **4**, 247 (2000).
[14] M.P. Mintchev, A. Girard, and K.L. Bowes, IEEE Trans. Biomed. Eng. **47**, 239 (2000).
[15] M.P. Mintchev and K.L. Bowes, Med. Biol. Eng. Comput. **36**, 7 (1998).
[16] P.Z. Rashev, K.L. Bowes, and M.P. Mintchev, IEEE Trans. Inf. Technol. Biomed. **6**, 296 (2002).
[17] M.P. Mintchev, S.J. Otto, and K.L. Bowes, Gastroenterology **112**, 2006 (1997).
[18] M.P. Mintchev and K.L. Bowes, Med. Eng. Phys. **20**, 177 (1998).
[19] J. Sarvas, Phys. Med. Biol. **32**, 11 (1987).
[20] R.J. Ilmoniemi, M.S. Hämäläinen, and J. Knuutila *Biomagnetism: Applications and Theory* (Pergamon, Oxford, 1985), pp. 278–282.
[21] J.C. Mosher, R.M. Leahy, and P.S. Lewis, in *Proceedings of the International Conference on Acoustics, Speech and Signal Processing, 1995* (IEEE Signal Processing Society, Detroit, MI, 1995), p. 2943.
[22] J.C. Mosher and R.M. Leahy, IEEE Trans. Signal Process. **47**, 332 (1999).
[23] Z.S. Wang, J.Y. Cheung, S.K. Gao, and J.D.Z. Chen, Methods Inf. Med. **39**, 186 (2000).
[24] L.A. Bradshaw, S.H. Allos, J.P. Wikswo, Jr., and W.O. Richards, Am. J. Physiol. **35**, G1159 (1997).